

Research Article

Sliding Mode Variable Structure Control and Real-Time Optimization of Dry Dual Clutch Transmission during the Vehicle's Launch

Zhiguo Zhao, Haijun Chen, and Qi Wang

School of Automotive Studies, Tongji University, Shanghai 201804, China

Correspondence should be addressed to Zhiguo Zhao; zhiguo Zhao@tongji.edu.cn

Received 19 September 2013; Revised 5 November 2013; Accepted 5 November 2013; Published 2 February 2014

Academic Editor: Hui Zhang

Copyright © 2014 Zhiguo Zhao et al. This is an open access article distributed under the Creative Commons Attribution License, which permits unrestricted use, distribution, and reproduction in any medium, provided the original work is properly cited.

In order to reflect driving intention adequately and improve the launch performance of vehicle equipped with five-speed dry dual clutch transmission (DCT), the issue of coordinating control between engine and clutch is researched, which is based on the DCT and prototype car developed independently. Four-degree-of-freedom (DOF) launch dynamics equations are established. Taking advantage of predictive control and genetic algorithm, target tracing curves of engine speed and vehicle velocity are optimally specified. Sliding mode variable structure (SMVS) control strategy is designed to track these curves. The rapid prototyping experiment and test are, respectively, conducted on the DCT test bench and in the chassis dynamometer. Results show that the designed SMVS control strategy not only effectively embodies the driver's intention but also has strong robustness to the vehicle parameter's variations.

1. Introduction

Based on the automated mechanical transmission (AMT), if remodelling its transmission mechanism (including input shaft, positions of gear pairs, and intermediate shaft) and adding a set of dry friction clutch and corresponding actuator, dry dual clutch transmission (DCT) can be constructed. The problem of traction interruption, while gear shifting, can also be resolved effectively through the coordinating control between two clutches and engine. So, the quality of shifting and the power performance of vehicle can also be improved.

As to the launch process of vehicle equipped with dry DCT, single or double clutches can be adopted to launch. Launching with double clutches aims at balancing the sliding friction work of twin clutches and lengthening their service life [1, 2], but dual clutches participation mode can easily lead to power cycling inside the DCT, so its feasibility requires further investigation. By contrast, when single clutch is involved, the launch dynamics model and control logic of DCT are the same as the AMT's, because the launch modelling and controlling of vehicle equipped with AMT have

been studied widely and profoundly. Two degree-of-freedom (DOF) dynamics model has been set up and the optimal clutch engaging control law via minimum principle has been founded [3, 4]. Quadratic optimal launch controller has been designed and equivalent damping of AMT transmission has also been taken into account [5, 6]. Six-DOF launch dynamics equations and clutch's hydraulic actuator model have been established. The corresponding model's parameters have been also obtained through experiments [7]. Five-DOF launch model has been established and simplified, and engine speed decoupling control strategy has also been put forward [8]. In addition, fuzzy logic control method for the launching process of AMT based on experience has been studied largely and fuzzy input variables could be the accelerator pedal opening and its changing rate [9], or the deviation and its changing rate between engine speed and target speed related to accelerator pedal [10], or the rotary speed difference between clutch driving plate and driven plate [11]. Generally, output variables could be clutch engaging speed; genetic algorithm has been further used to optimize the fuzzy rule set [12]. Moreover, in the aspect of launch control for vehicle

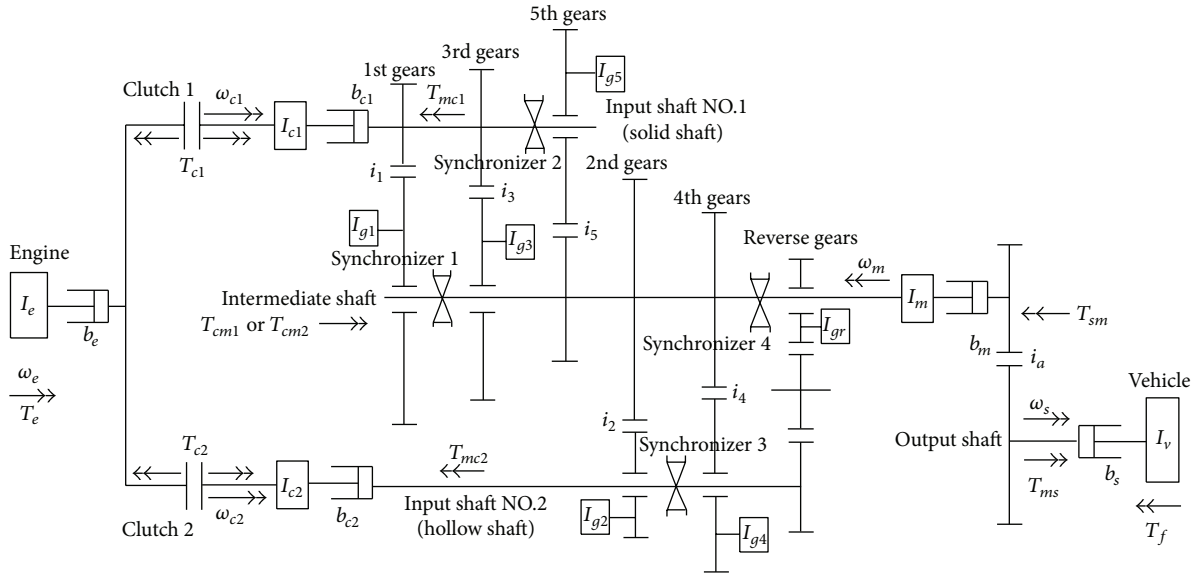


FIGURE 1: Five-speed dry DCT dynamic model.

equipped with DCT, clutch optimal engaging control law has been introduced by utilizing minimum principle and synthetically taking shock intensity, sliding friction work, and engine output torque into consideration [13]. Linear quadratic optimal control has been applied to simulate clutch engaging pressure in the launching process [14, 15]. Launch fuzzy intelligent control algorithm has been designed and optimized by using accelerator pedal opening and its changing rate, clutch relative slip rate and engine speed difference to describe the driving intention, clutch engaging states and engine working condition, respectively [16]. Comparatively, double-layer fuzzy intelligent control architecture has been presented by setting up clutch engaging fuzzy control rules and real car chassis dynamometer test has been conducted [17].

But the above stated studies only focus on the control of clutch engaging control rules, rarely taking consideration of the issue of coordinating control between engine and clutch during the vehicle's launch process and let alone the qualification of driver's intention.

Taking the factors such as driver's intention, engine condition, clutch state, and shock intensity into account, the issue of coordinating control between engine and clutch is investigated in the paper, which is based on the DCT and prototype car developed independently. Four degrees of freedom (DOF) launch dynamics equations are established. The computational formulas of engine speed and clutch transfer torque in the launching process have also been quantified and given. Taking advantage of predictive control and genetic algorithm, target tracing curves of engine speed and vehicle velocity are optimally specified. Sliding mode variable structure (SMVS) control strategy has been designed to track these curves. Based on the Matlab/Simulink software platform and the hardware-in-the-loop test bench, the launch performance of prototype car equipped with dry DCT has been simulated under different driving conditions, and the rapid prototyping

experiment and test are, respectively, conducted on the DCT test bench and in the chassis dynamometer.

2. Mathematical Models

2.1. Five-Speed Dry DCT Dynamic Model. The five-speed dry DCT described in the paper is made up of dry dual clutch module and its actuator, four synchronizers and their actuators, and single intermediate shaft gear transmission mechanism. In order to study the dynamic characteristic of single clutch in the launching process and develop relevant coordinating control strategy, the following assumptions should be made before modeling (1) Both wheels' moment of inertia and vehicle's translation quality are converted into the transmission output shaft. The engine output shaft and the input shaft, intermediate shaft, and output shaft of transmission are regarded as rigid body with distributed parameters and concentrated inertia, and the friction damping loss is considered, respectively (2) The dynamic process of the clutch actuator and the synchronizers, as well as the heat fade of the clutch are not the focus of this paper. (3) Neglect the elasticity between bearing and its block, as well as the elasticity and gap in gear engagement. Finally the established dynamic model of five-speed dry DCT after simplification is shown in Figure 1.

In Figure 1, parameters and variables are defined as follows:

I_e : equivalent moment of inertia of engine crankshaft (including flywheel) and clutch driving plate;

I_{c1} : Equivalent moment of inertia of clutch 1 driven plate, transmission NO.1 input shaft (solid part), and relevant odd number gears;

I_{c2} : equivalent moment of inertia of clutch 2 driven plate, transmission NO.2 input shaft (hollow part) and its relevant even number speed gears;

I_m : equivalent moment of inertia of transmission intermediate shaft, its relevant gears, and final drive driving part;

I_s : equivalent moment of inertia of final drive driven part, differential gears, axle shafts, wheels, and complete vehicle, which are equally converted into transmission output shaft;

I_{g1}, I_{g3}, I_{gr} : moment of inertia of 1st, 3rd, and reverse driven gears;

I_{g2}, I_{g4}, I_{g5} : moment of inertia of 2nd, 4th, and 5th driving gears;

$i_1 \sim i_5, i_a$: forward gear ratios and final drive ratio;

b_e : rotating viscous damping coefficient of engine output shaft;

b_{c1} : rotating viscous damping coefficient of transmission NO.1 input shaft;

b_{c2} : rotating viscous damping coefficient of transmission NO.2 input shaft;

b_m : rotating viscous damping coefficient of transmission intermediate shaft;

b_s : equivalent rotating viscous damping coefficient of axle shafts and wheels, which are equally converted into transmission output shaft;

ω_e : angular speed of engine crankshaft;

ω_{c1} : angular speed of clutch 1 driven plate (or transmission NO.1 input shaft);

ω_{c2} : angular speed of clutch 2 driven plate (or transmission NO.2 input shaft);

ω_m : angular speed of transmission intermediate shaft;

ω_s : angular speed of transmission output shaft;

T_e : engine output torque;

T_{c1}, T_{c2} : transfer torque of clutch 1 and clutch 2;

T_{cm1}, T_{cm2} : torque of NO.1 and NO.2 input shafts acting on intermediate shaft;

T_{mc1}, T_{mc2} : torque of intermediate shaft reacting on NO.1 and NO.2 input shafts;

T_f : driving resistance torque which is equally converted into transmission output shaft.

2.2. Dynamics Equations for Five-Speed Dry DCT. DCT can use 1st speed gear or 2nd speed gear to start. Take 1st speed gear launch for example. Assuming that the engine is already operating in idle state, the synchronizer 1 firstly engages to the left gear (1st gear). Because the synchronizer engaging process does not belong to the research focus in this paper, the detailed analysis of synchronizer is neglected. After the engagement of synchronizer, the clutch 1 begins to engage to transmit the torque from the engine side until the end of

launching process. During the launch process, clutch 1 gets through four phases.

Free Stroke Eliminating. It is to eliminate the vacant distance between the clutch driving and driven plates.

Slipping Friction before Half-Engaging. The clutch begins to engage but the transmitted torque cannot overcome the vehicle resistance to move the vehicle.

Sliding Friction after Half-Engaging. The clutch is further engaged and the torque transmitted by clutch is able to force the vehicle to move.

Full-Engaging after Synchronizing. The engaging process and the launching process finish.

The first two phases have a small effect on the launching quality and therefore the main research attention is focused in the last two phases, especially the third phase.

The four-DOF dynamics equations on the phase of slipping friction after half-engaging can be expressed as follows:

$$I_e \dot{\omega}_e = T_e - T_{c1} - b_e \omega_e,$$

$$I_{c1} \dot{\omega}_{c1} = T_{c1} - T_{mc1} - b_{c1} \omega_{c1},$$

$$(I_m + I_{g1} + I_{g2} i_2^2 \eta + I_{g4} i_4^2 \eta + I_{g5} i_5^2 \eta) \dot{\omega}_m \quad (1)$$

$$= T_{c1m} - T_{sm} - b_m \omega_m,$$

$$I_s \dot{\omega}_s = T_{ms} - T_f - b_s \omega_s,$$

where $T_e = f(\alpha, \omega_e)$, $T_{cm1} = T_{mc1} i_1 \eta$, $T_{ms} = T_{sm} i_a \eta$, $v = \omega_s R_W$

$$T_{c1} = \begin{cases} \frac{2}{3} \left(\frac{R_0^3 - R_1^3}{R_0^2 - R_1^2} \right) \mu_1 F(x_1) & \omega_{c1} \leq \omega_e, \\ T_{c1}^L & \omega_{c1} = \omega_e, \end{cases} \quad (2)$$

$$T_f = \left(\frac{C_d A}{21.15} v^2 + mg \sin \theta + mg \cos \theta f + \delta m \frac{dv}{dt} \right) R_W, \quad (3)$$

$$\delta = 1 + \frac{1}{m} \frac{I_{c1} i_1^2 i_a^2 + I_m i_a^2 + I_s + I_v}{R_W}. \quad (4)$$

Among above formulas, α is engine throttle opening. $f(\alpha, \omega_e)$ denotes nonlinear function of engine output torque. η is transmitting efficiency of transmission shafts as well as final drive. μ_1 is kinetic friction coefficient among friction plates of clutch 1. R_0, R_1 are internal and external radius of friction plates of clutch 1. x_1 is opening of clutch 1. $F(x_1)$ denotes positive pressure function of pressure plate of clutch 1. T_{c1}^L is transfer torque after full-engaging of clutch. m is vehicle mass. g is gravity acceleration. f is rolling resistance coefficient. v is vehicle velocity. C_d is wind drag coefficient. A is windward area. θ is road slope. δ is conversion coefficient of rotating mass. R_W is radius of wheel.

For the sake of easily designing the controller, further assumptions about motional relationship among the input, intermediate, and output shafts of transmission should meet the equations $\omega_s i_a i_1 = \omega_m i_1 = \omega_{c1}$. Then the DCT dynamic model in Figure 1 can be simplified as that in Figure 2.

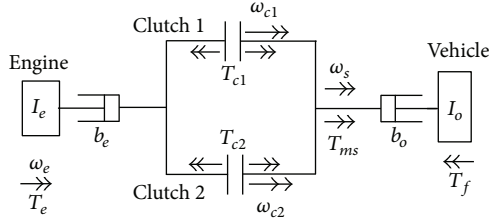


FIGURE 2: DCT dynamics model after simplification.

Simplify formula (1), and then some two-DOF dynamics equations are obtained:

$$I_e \dot{\omega}_e + b_e \omega_e = T_e - T_{c1}, \quad (5)$$

$$I_o \dot{\omega}_s + b_o \omega_s = T_{c1} i_e - T_f,$$

where parameters are defined as follows:

$$\begin{aligned} i_e &= i_a i_1 \eta^2 \\ I_o &= I_s + (I_m + I_{g1}) i_a^2 \eta + I_{c1} i_1^2 i_a^2 \eta^2 + I_{g2} i_2^2 i_a^2 \eta^2 \\ &\quad + I_{g4} i_4^2 i_a^2 \eta^2 + I_{g5} i_5^2 i_a^2 \eta^2, \\ b_o &= b_s + b_m i_a^2 \eta + b_{c1} i_1^2 i_a^2 \eta^2. \end{aligned} \quad (6)$$

When the clutch is fully engaged, $T_{c1} = T_{c1}^L$. He clutch transmitted torque T_{c1} is only determined by engine output torque and driving resistance, which satisfies:

$$T_{c1} = \frac{I_o (T_e - b_e \omega_e) + (T_f + b_o \omega_s) I_e i_1 i_a}{I_o + I_e i_e i_1 i_a}. \quad (7)$$

When the clutch is fully engages, the vehicle is launched in certain gear. In this sense, formula (5) can still be further simplified as a single-DOF dynamics equation:

$$I_d \dot{\omega}_s + b_d \omega_s = T_e i_e - T_f, \quad (8)$$

where

$$\begin{aligned} I_d &= I_s + (I_m + I_{g1}) i_a^2 \eta + (I_{c1} + I_e) i_1^2 i_a^2 \eta^2 \\ &\quad + I_{g2} i_2^2 i_a^2 \eta^2 + I_{g4} i_4^2 i_a^2 \eta^2 + I_{g5} i_5^2 i_a^2 \eta^2, \\ b_d &= b_s + b_m i_a^2 \eta + (b_{c1} + b_e) i_1^2 i_a^2 \eta^2. \end{aligned} \quad (9)$$

Synthesizing formulas (5) and (8), the DCT launch dynamic model after eliminating the null distance of clutch can be seen as a hybrid model, namely including a two-DOF sliding friction model and a single-DOF stably operated model. The switching condition between the two models is $\omega_e = \omega_{c1}$. The controller will be designed on the basis of this hybrid model in the following.

3. Coordinating Control and Real-Time Optimization for Dry DCT

3.1. Launch Control Objectives. The control objectives of dry DCT in the launching process are as follows:

- (1) reflect the driver's intention adequately to let the driver have different driving feel according to accelerator pedal opening and its changing rate;
- (2) under the condition of meeting the requirements of shock intensity and sliding friction work, to decrease the slipping friction work as much as possible and guarantee the launch comfort (shock intensity is 10 m/s^3 in German standard [18]);
- (3) take the effect of launching on engine's working state into account to avoid the flameout of the engine in the launching process.

3.2. Launch Controller Design Architecture. A layered architecture of launching control is used as shown in Figure 3. The upper layer controller is applied to determine the optimal clutch transfer torque and engine target speed (or torque), while the lower one is used to implement a servocontrol of clutch torque and a closed-loop control of engine torque (or speed). The upper controller can further be divided into two parts according to the activation order: the sliding control before the speed synchronization and engaging control after the speed synchronization. The sliding control is aiming at the sliding friction after half-engaging phase and also the core of the launching control. Based on the two-DOF model during the sliding phase, the driving intention, the closed-loop control of engine speed and clutch torque, and can be realized. Relatively, based on the single-DOF model, the engaging control is for the full-engaging after synchronizing phase and to make the clutch engage completely as quickly as possible and prevent engaged clutch plates from falling into sliding state again due to the change of engine output torque. Meanwhile, engine output torque is adjusted to match the demand torque. Even though the driving and driven plates are already synchronized, the launch controller does not send out an accomplishment signal. Only if the engine output torque is equal to the demand torque, it sends out the signal.

3.3. Launch Sliding Friction Process Control. The inputs of launch slipping friction process control include accelerator pedal opening, engine speed, wheel speed, and so forth. The outputs contain Clutch 1 target engaging pressure and engine demand torque. They would be realized through the sliding mode variable structure tracing control algorithm.

(1) Determine target control variables. The target control variables include engine target speed and vehicle target shock intensity. The engine target speed should be proportional to the accelerator pedal opening and its changing rate in order to partially reflect the driver's intention. Taking engine target speed and vehicle target shock intensity as measuring index of driver's intention, the DCT launch controller can be designed without considering the concrete physical characteristics of clutch actuators, thus improving the generality of launch controller.

(2) Target tracing controller design. Based on simplified models of engine and transmission, sliding mode variable

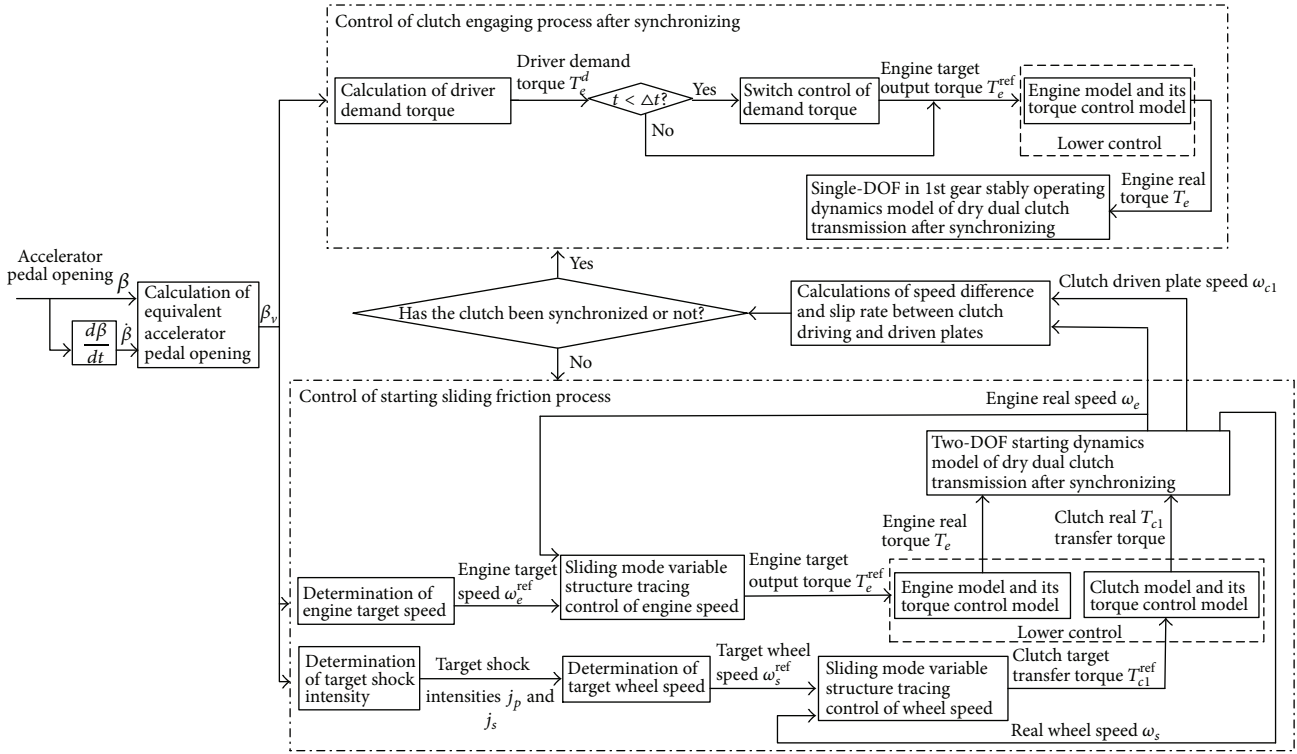


FIGURE 3: Design architecture of launch controller.

structure controller is designed to track engine target speed and vehicle target shock intensity.

3.3.1. *Determining Method of Engine Target Speed.* The principles of determining engine target speed are as follows.

- (1) In order to avoid the stalling of engine and attrition of clutch due to overhigh speed, the target speed is not less than the engine idle speed (set as 800 r/min) and is limited to a maximum value (set as 2000 r/min) as well.
- (2) Within optional limits of target speed, on one hand, the target speed changes along with the variation of accelerator pedal opening and its changing rate, and it can ensure that engine has enough output power to meet the launch demands under different conditions. On the other hand, the selected target speed can make the engine work in an economic area.
- (3) When the difference between engine real speed and clutch driven plate speed is more than the setting threshold value $\Delta\omega$ and the clutch sliding friction time is less than the time variable t_p , the engine target speed will coordinate with the accelerator pedal opening and its changing rate. If the condition is reverse, the target speed will be fixed as synchronous speed $\omega_e(t_s)$, namely, the speed when engine and clutch driven plate are at the moment of synchronizing. The calculation of engine target speed ω_e^{ref} is shown

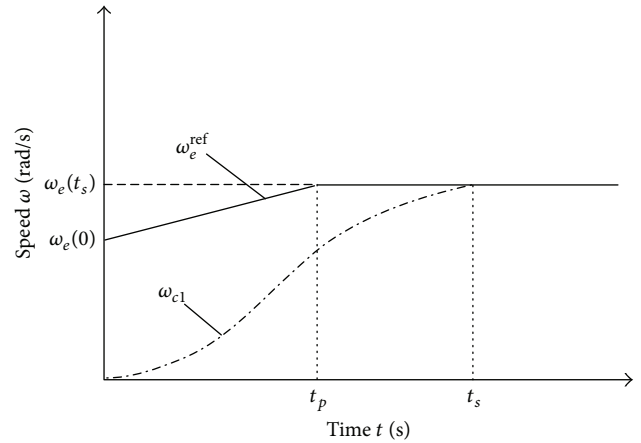


FIGURE 4: Determination of engine target speed.

in Figure 4 and Formula (10). The engine output characteristic can be seen in Figure 15. Consider

$$\omega_e^{ref} = \begin{cases} \frac{\omega_e(t_s) - \omega_e(0)}{t_p} t + \omega_e(0) & (\omega_e - \omega_{c1}) \geq \Delta\omega, t < t_p, \\ \omega_e(t_s) & \text{other,} \end{cases} \quad (10)$$

where $\omega_e(t_s)$ and $\omega_e(0)$, respectively, denote engine target speed postsynchronizing and idle speed. t_p is linearly increasing time of engine speed. t_s is time elapsed until clutch driving

TABLE 1: Engine synchronous target speed.

Equivalent accelerator pedal opening $\beta_v/\%$	Engine synchronous target speed $\omega_e(t_s)/(r/\min)$
0~10	1000
10~20	1000
20~30	1100
30~40	1200
40~50	1300
50~60	1400
60~70	1500
70~80	1600
80~90	1700
90~100	2000

and driven plates are synchronized. $\Delta\omega$ is set threshold value of the difference between clutch driving and driven plates.

In order to reflect the driver's intention easily and determine $\omega_e(t_s)$, equivalent accelerator pedal opening β_v is introduced to synthesize the information of accelerator pedal opening and its changing rate. The relationship between β_v and $\omega_e(t_s)$ is shown in Table 1.

Consider

$$\beta_v(t) = \beta(t) + k\dot{\beta}(t), \quad (11)$$

where $\beta(t)$ is real value of accelerator pedal opening. $\dot{\beta}(t)$ is changing rate of accelerator pedal opening. k is weight index and must be determined according to the practice to guarantee the $\beta_v(t)$ falling into the scope of [0–100].

3.3.2. Determining Method of Target Shock Intensity in the Launching Process. The launch target shock intensity not only reflects the driver's intention, but also guarantees that the intensity is in a reasonable extent. The friction process is divided into three parts in [19], which qualitatively elaborated control key points when a vehicle was launched and its clutch driving and driven plates were synchronizing. In [20], the shock intensity while the clutch driving and driven plates were synchronizing is derived, which showed that it is proportional to the difference between engine acceleration and acceleration of clutch driven plate at the instant of presynchronization. That is

$$\dot{\omega}_c(+)-\dot{\omega}_c(-)=\frac{I_e}{I_e+I_{ca}}[\dot{\omega}_e(-)-\dot{\omega}_c(-)], \quad (12)$$

where $\dot{\omega}_c(-)$, $\dot{\omega}_c(+)$ denote accelerations of clutch driven plate at the instant of presynchronization and post-synchronization. $\dot{\omega}_e(-)$ is engine acceleration at the instant of presynchronization. I_{ca} is moment of inertia of complete vehicle and its transmission system, which are equally converted to clutch driven plate.

Suppose that the transmission system is rigid; namely, $\dot{v} = \dot{\omega}_s R_W = \dot{\omega}_c i_a R_W$. The shock intensity of vehicle can

TABLE 2: Driver's intention.

Launch mode	Slow	Moderate	Abrupt
Equivalent accelerator pedal opening $\beta_v/\%$	0~20	20~50	50~100
Target shock intensity $j_p/(m/s^3)$	0.5	1.5	2.5

be equally converted into the shock intensity of clutch driven plate. Consider Formula (12). If the difference between engine acceleration and acceleration of clutch driven plate is zero, the shock intensity will be zero at the moment of synchronizing. The condition is called no-impact synchronizing condition. As the engine target speed is determined in preceding passage, namely, the rotary speed difference is less than the threshold value $\Delta\omega$ or the elapsed time of sliding friction process is more than the time variable t_p , the engine speed remains constant as the same as synchronous target speed. So the engine acceleration is zero. For the sake of no-impact at the moment of synchronizing, the speed of clutch driven plate should be equal to the target speed and its acceleration should be zero.

The authors divide the launch sliding friction process into three phases, determine the target shock intensity in different phases, and obtain related target vehicle acceleration and target vehicle velocity via integral. It is shown in Figure 5.

Phase One. During the time slot $0 \sim t_p$, the target shock intensity j_p is positive. It changes along with the equivalent acceleration, which reflects the driver's intention. As the particularity of creeping launch, that is, the clutch driving and driven plates should maintain slipping state during the whole launching process without considering their speed synchronization. In view of this, creeping launch is out of consideration in this paper. Therefore, on the basis of equivalent accelerator pedal opening and engine output torque capacity, driver's intention is divided into three categories [3, 6], which is shown in Table 2.

Phase Two. During the time slot $t_p \sim t_s$, the target shock intensity j_p is negative. The main goal is to lower the vehicle acceleration, so that the speed and acceleration of clutch driven plate stay the same as the engine's at the moment of synchronizing in order to realize no-impact synchronizing. The values are synchronous target speed and zero, respectively. Theoretically, different values are selected according to different target shock intensity in Phase One. However, considering that clutch driving plate and its driven plate are approaching to synchronize, the target shock intensity j_s is set as a constant value in order to accelerate the engaging speed and decrease the total sliding friction work in the launching process. Equations can be established as follows:

$$\begin{aligned} j_p t_p + j_s (t_s - t_p) &= 0, \\ 0.5 j_p t_p^2 + j_p t_p (t_s - t_p) + 0.5 j_s (t_s - t_p)^2 &= \omega(t_s) R_W, \end{aligned} \quad (13)$$

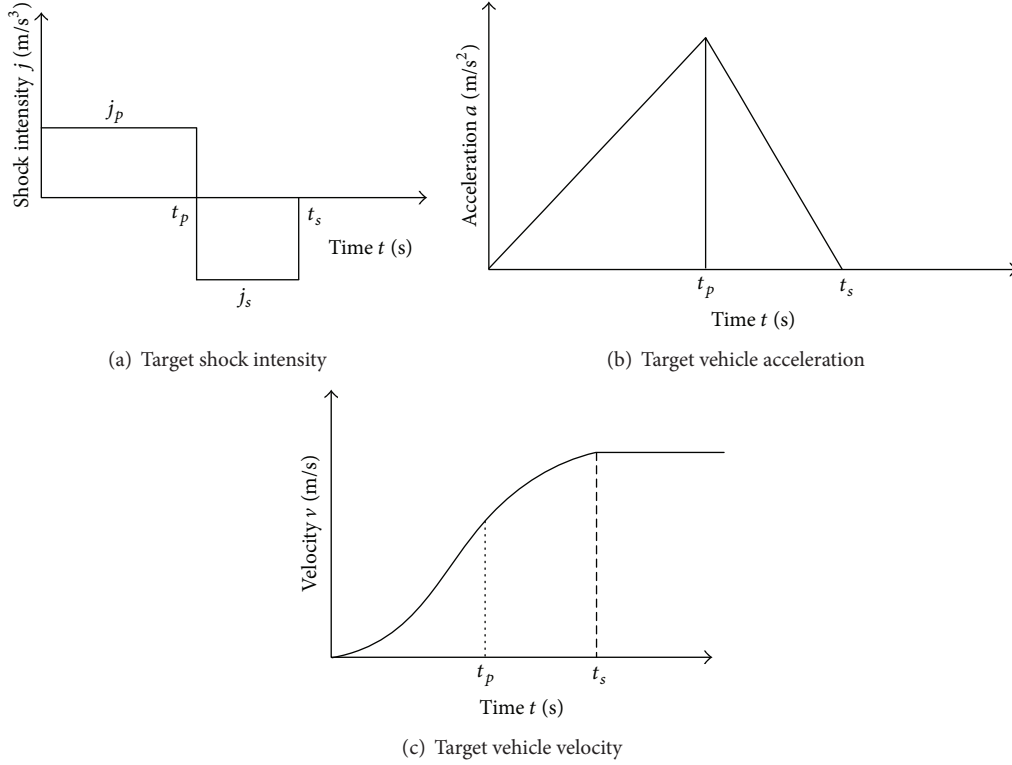


FIGURE 5: Target curves in the launching process.

where j_p is target shock intensity in phase one of sliding friction process, j_s is target shock intensity in Phase Two of sliding friction process. $\omega(t_s)$ is speed of clutch driven plate at time t_s , namely, the synchronous target speed.

By solving formula (13), the following can be obtained:

$$t_p = \sqrt{\frac{\omega(t_s) R_W}{(0.5j_p - 0.5j_p^2/j_s)}}, \quad (14)$$

$$t_s = t_p \left(1 - \frac{j_p}{j_s} \right).$$

According to equivalent accelerator pedal opening at the initial moment of sliding friction process, the synchronous target speed and target shock intensity in Phase One can be obtained by looking up Tables 1 and 2, respectively. Based on above values t_p and t_s , the target speed of clutch 1 in the sliding friction process will be listed in the following through the integral of j_p and j_s twice:

$$\omega_s^{\text{ref}} = \int_0^{t_s} \int_0^{t_s} \frac{j}{R_W} dt, \quad (15)$$

$$\omega_{c1}^{\text{ref}} = \omega_s^{\text{ref}} t_1 i_a.$$

Note that both t_p and t_s are measured in a coordinate system whose origin is the initial moment of sliding friction process.

Phase Three. During the time slot over t_s , clutch driving plate and its driven part are already synchronized, and DCT model is switched from sliding friction model to 1st speed gear stably operated model. So the control of sliding friction makes no sense any more. In order to meet the requirement of no-impact synchronizing, the target acceleration is set as zero and the target speed is constant.

3.3.3. Rolling Determination of Target Value and Genetic Optimization of Shock Intensity. The determining method of engine target speed and launch target shock intensity stated above can ensure no stalling of engine and ride comfort of vehicle in the launching process and partially reflect the driver's intention, but some shortages also exist as follows.

- (1) Engine synchronizing target speed and target shock intensity in Phase One are only based on equivalent accelerator pedal opening at the initial moment of sliding friction process, without considering the whole sliding friction process. The transformation of equivalent accelerator pedal opening obviously does not accord with the fact.
- (2) Neglect the sliding friction work in the launching process when determining the target speed.

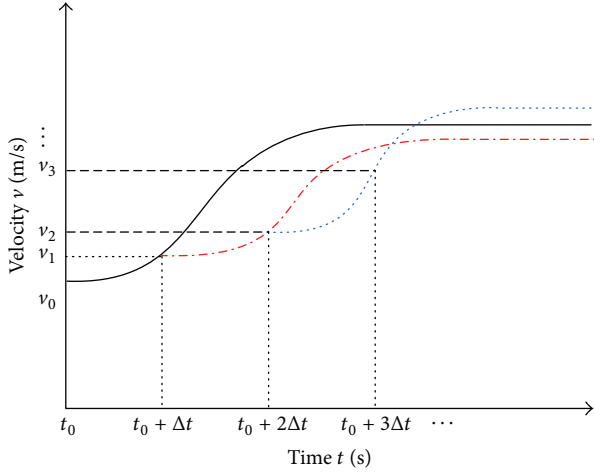


FIGURE 6: Schematic diagram of the rolling calculation of launch target vehicle velocity.

In order to overcome the above shortages, predictive control thoughts are used to optimize the target curves online. It means that during a time slot (namely, at an optimizing step), these variables, such as $\omega_e(t_s)$, t_p , t_s , and j_p can be obtained by minimizing the sliding friction work on the basis of the equivalent accelerator pedal opening and vehicle velocity. And then the target curves can also be obtained.

Determination of Rolling Algorithm of Target Vehicle Velocity. The target vehicle velocity curve is recalculated in a time interval Δt . Both vehicle velocity and acceleration are not equal to 0 at every calculation moment. Figure 6 shows that v_0 , v_1 , v_2 , and v_3 represent the target vehicle velocities at these moments of t_0 , $t_0 + \Delta t$, $t_0 + 2\Delta t$, and $t_0 + 3\Delta t$, respectively.

Figure 7 shows the calculation method of target vehicle velocity in a certain time. According to the condition of no-impact synchronizing, formula (13) can be rewritten as:

$$\begin{aligned} a(t_0) + j_p t_p + j_s(t_s - t_p) &= 0, \\ v(t_0) + a(t_0)t_p + \frac{1}{2}j_p t_p^2 + (\alpha(t_0) + j_p t_p)(t_s - t_p) & \quad (16) \\ + \frac{1}{2}j_s(t_s - t_p)^2 &= \omega(t_s)R_W, \end{aligned}$$

where t_0 is optimizing moment, $\alpha(t_0)$ denotes vehicle acceleration at the optimizing moment, $v(t_0)$ denotes vehicle velocity at the optimizing moment, and $\omega_e(t_s)$ denotes synchronous target revolving speed, which updates its value at every optimizing step according to virtual accelerator pedal signal by looking up Table 1.

In a word, firstly at every optimizing step, synchronous target rotary speed $\omega_e(t_s)$ and target shock intensity are obtained by looking up Tables 1 and 2 according to the current equivalent accelerator pedal opening. Secondly solve (16) and get the latest values of t_p , t_s . Finally according to formula (15), we get the target vehicle velocity in the launching process.

The rolling determining method of engine target speed resembles the above description. According to (10), following formula can be obtained:

$$\omega_e^{\text{ref}} = \begin{cases} \frac{\omega_e(t_s) - \omega_e(0)}{t_p} t + \omega_e(0), & (\omega_e - \omega_{c1}) \geq \Delta\omega, \\ \omega_e(t_s), & \text{other.} \end{cases} \quad t_0 < t < (t_0 + t_p), \quad (17)$$

Determination of Optimal Algorithm of Target Shock Intensity. The target shock intensity stated above is obtained by looking up Tables. But it does not ensure that the target curve is optimal. It is discussed below how to determine j_p and j_s through genetic algorithm and real-time optimization. In the time slot $t_0 \sim t_0 + t_s$, the predictive sliding friction work is

$$W = \int_{t_0}^{t_0+t_s} \hat{T}_{c1} (\omega_e^{\text{ref}} - \omega_{c1}) dt, \quad (18)$$

$$\hat{T}_{c1} = \frac{I_o \dot{\omega}_s^{\text{ref}} + b_o \omega_s^{\text{ref}} + mgR_W \mu}{i_a^2 i_1 \eta^2},$$

where \hat{T}_{c1} is estimated clutch transfer torque. If $|T_{c1} - \hat{T}_{c1}| < \varepsilon$, estimated value \hat{T}_{c1} replaces real value T_{c1} , and target shock intensities j_p and j_s can be obtained by minimizing the sliding friction work. The selected fitness function based on genetic algorithm is the reciprocal of predictive sliding friction work:

$$F = \frac{1}{W}. \quad (19)$$

The optimizing process of parameters j_p and j_s can be seen in Figure 8.

3.3.4. Design of Sliding Mode Variable Structure Tracing Controller. Based on the design of previous details, the target vehicle velocity and target engine speed are already obtained in the launch sliding friction process. However, whether it can track accurately or not, depends on the performance of launch controller completely. Considering immeasurable driving resistance, a kind of sliding mode variable structure control algorithm with interference rejection has been put forward in the paper, which aims at tracking engine speed and wheel speed accurately.

Regardless of the influence of temperature and slip speed difference on clutch friction coefficient μ_1 , the relationship between pressure F_1 of the clutch pressure plate and its transfer torque is determined uniquely, when the internal and external radius of friction plates are given. For the sake of easy description, clutch transfer torque is used to describe the clutch engaging law in the following.

Tracing Control of Wheel Speed. On the basis of launch dynamics equations of DCT transmission system (referring to Formula (5)), supposing $x_1 = \theta_s$, $x_2 = \omega_s$, there is:

$$\begin{aligned} \dot{x}_1 &= x_2, \\ \dot{x}_2 &= \frac{i_e}{I_o} T_{c1} - \frac{b_o}{I_o} x_2 - \frac{T_f}{I_o}. \end{aligned} \quad (20)$$

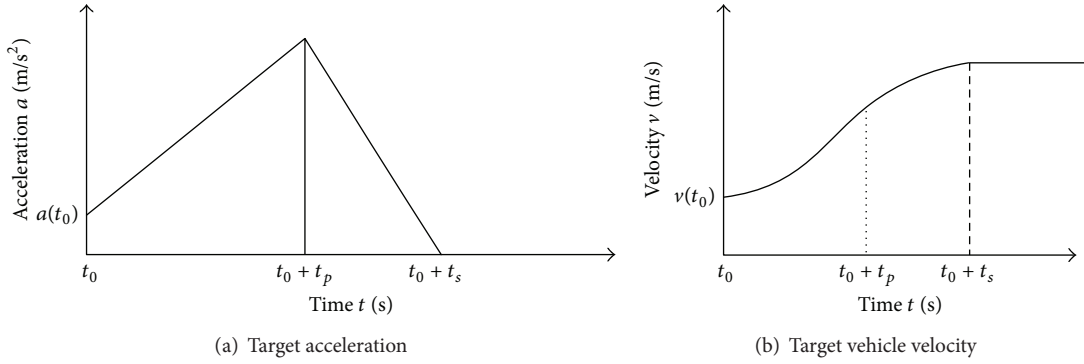
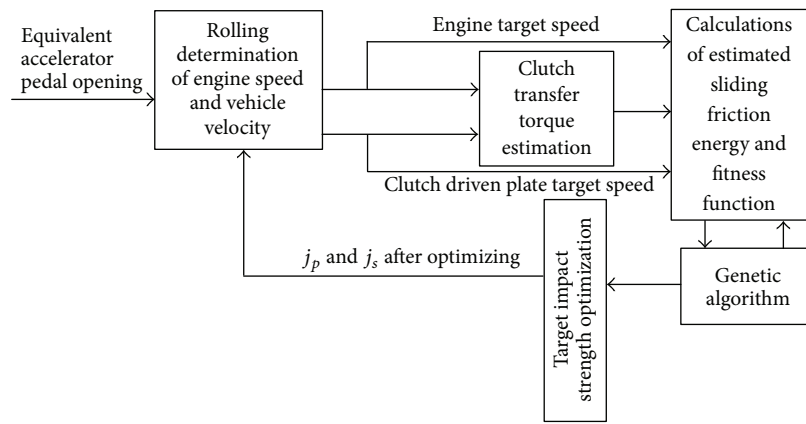

 FIGURE 7: Calculation schematic diagram of target vehicle velocity at time t_0 .


FIGURE 8: Optimizing process of target shock intensity.

Supposing that $e_1 = x_r - x_1$, $e_2 = \dot{x}_r - x_2$, $u_1 = T_{c1}$, where x_r is the expectation of x_1 , there is

$$\begin{bmatrix} \dot{e}_1 \\ \dot{e}_2 \end{bmatrix} = \begin{bmatrix} 0 & 1 \\ 0 & -\frac{b_0}{I_0} \end{bmatrix} \begin{bmatrix} e_1 \\ e_2 \end{bmatrix} + \begin{bmatrix} 0 \\ -\frac{i_e}{I_0} \end{bmatrix} u_1 + \begin{bmatrix} 0 \\ f_2 \end{bmatrix} + \begin{bmatrix} 0 \\ f_3 \end{bmatrix}, \quad (21)$$

where $f_2 = \ddot{x}_r + (I_0/b_0)\dot{x}_r$, which is measurable interference, and $f_3 = T_f/I_0$, which is immeasurable interference related to the driving resistance.

In order to reduce the gain of sliding mode variable structure, it should contract the upper and lower boundaries of interference as much as possible. According to the computational formula of driving resistance, the rolling resistance is regarded as a part of measurable interference; namely, measurable interference f_2 can be rewritten as

$$f_2' = \ddot{x}_r + \frac{I_0}{b_0}\dot{x}_r + \frac{mgf}{b_0}. \quad (22)$$

And the immeasurable interference f_3 can be rewritten as

$$f_3' = \frac{T_f}{I_0} - \frac{mgf}{b_0}. \quad (23)$$

The switching function is designed as

$$s = c_1 e_1 + c_2 e_2, \quad (24)$$

where $c_1 > 0$, $c_2 > 0$. Take the approaching rate:

$$\dot{s} = -k \cdot s - d \cdot g(s) + c_2 f_3', \quad (25)$$

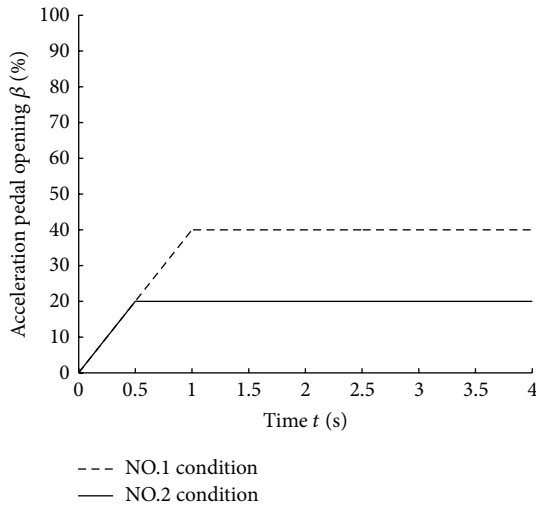
where $d > |c_2 f_3'|$,

$$g(s) = \begin{cases} \text{sgn}(s) & |s| \geq \frac{\pi}{2p} \\ \sin(p \cdot s) & |s| < \frac{\pi}{2p} \end{cases} \quad p > 0. \quad (26)$$

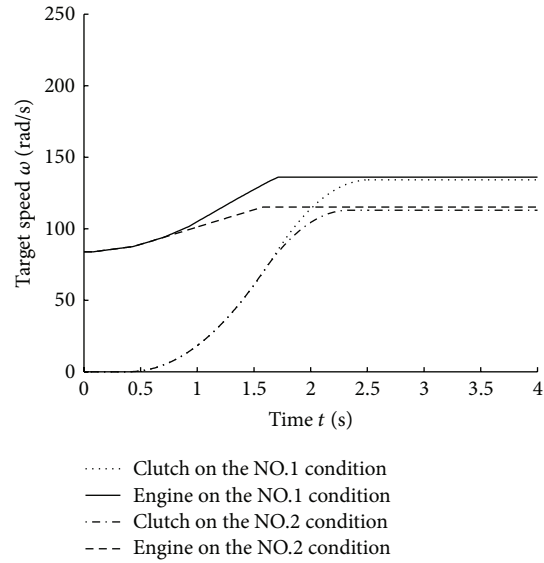
While it is $p \rightarrow \infty$, $g(s) \rightarrow \text{sgn}(s)$. The control input u_1 is calculated via the formula below:

$$u_1 = \frac{I_0}{c_2 i_e} \left[k \cdot s + d \cdot g(s) + e_2 \left(c_1 - c_2 \frac{b_0}{I_0} \right) + c_2 f_2' \right]. \quad (27)$$

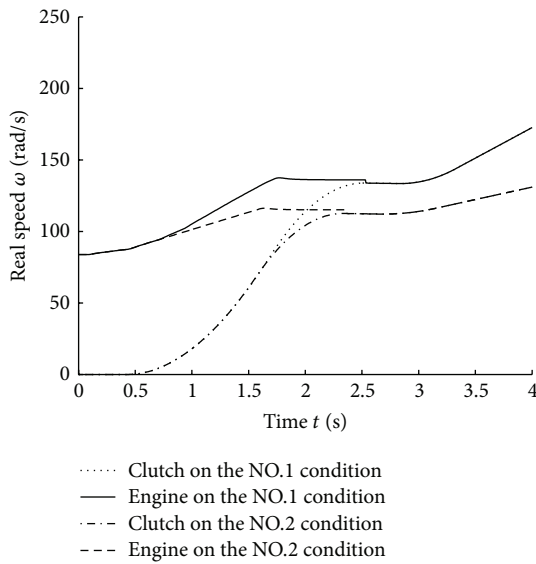
Tracing Control of Engine Speed. Because engine model is a double-input (T_e and T_{c1})-single-output (ω_e) model and clutch transfer torque T_{c1} is available in use of wheel speed tracing controller stated previously, T_{c1} is a measurable interference of engine model. Based on the rotation dynamics of crankshaft (refer to Formula (5)), we can suppose that



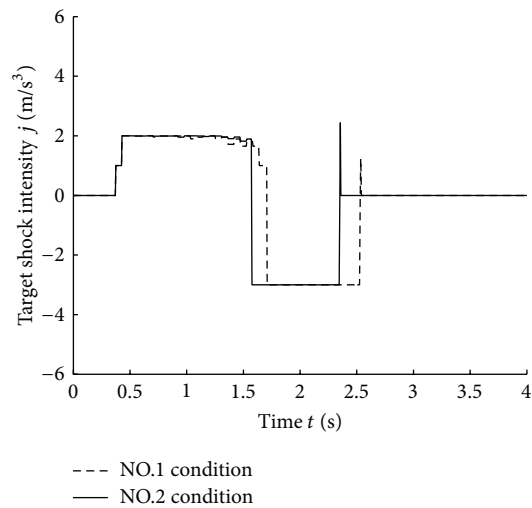
(a) Acceleration pedal opening value



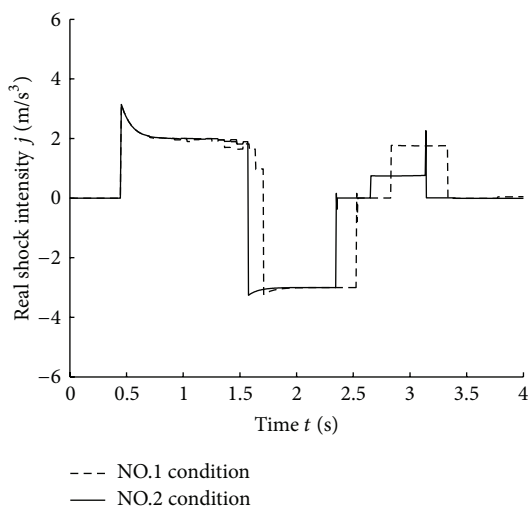
(b) Target rotational speed



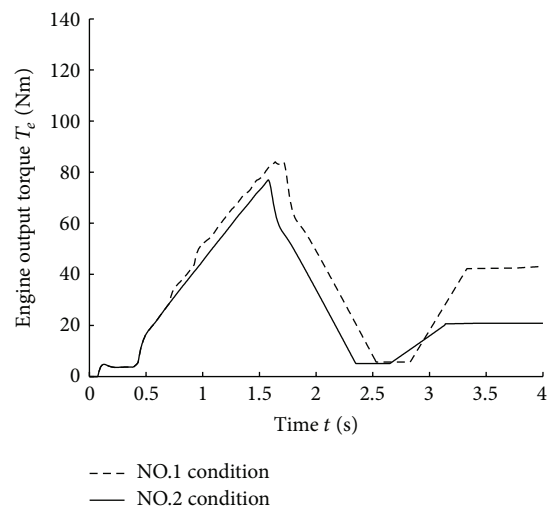
(c) Actual rotational speed



(d) Target impact strength



(e) Actual impact strength



(f) Engine output torque

FIGURE 9: Continued.

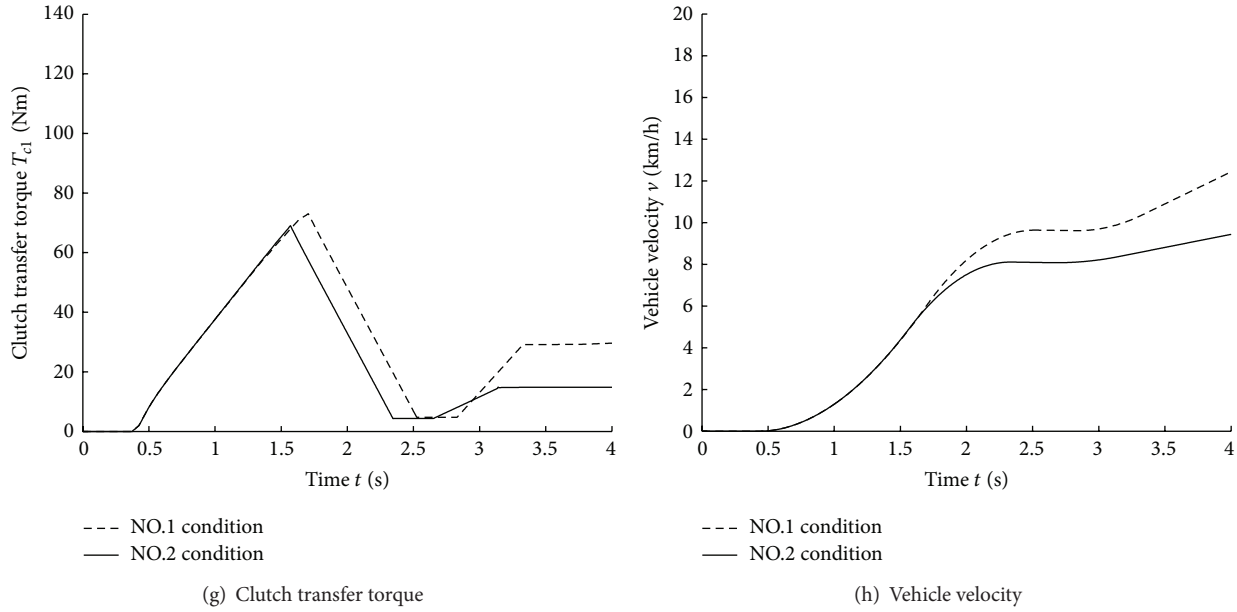


FIGURE 9: Simulation results of launch performance.

$x_{1e} = \theta_e$, $\dot{x}_{1e} = \dot{\theta}_e = \omega_e$, $e_{1e} = x_{re} - x_{1e}$, $e_{2e} = \dot{x}_{re} - \dot{x}_{2e}$, where x_{re} is the expectation of θ_e ; namely,

$$\begin{bmatrix} \dot{e}_{1e} \\ \dot{e}_{2e} \end{bmatrix} = \begin{bmatrix} 0 & 1 \\ 0 & -\frac{b_e}{I_e} \end{bmatrix} \begin{bmatrix} e_{1e} \\ e_{2e} \end{bmatrix} + \begin{bmatrix} 0 \\ -\frac{1}{I_e} \end{bmatrix} u_2 + \begin{bmatrix} 0 \\ f_{2e} \end{bmatrix}, \quad (28)$$

where $u_2 = T_e$, $f_{2e} = (T_{c1}/I_e) + \ddot{x}_{re} + (b_e/I_e)\dot{x}_{re}$, which are measurable interferences.

The switching function is designed as

$$s_e = c_{1e}e_{1e} + c_{2e}e_{2e}, \quad (29)$$

where $c_{1e} > 0$, $c_{2e} > 0$. Take the approaching rate:

$$\dot{s}_e = -k_e \cdot s_e - d_e \cdot g(s_e), \quad (30)$$

where $d_e > |c_{2e}f_{2e}|$,

$$g(s) = \begin{cases} \operatorname{sgn}(s), & |s| \geq \frac{\pi}{2p_e}, \\ \sin(p_e \cdot s), & |s| < \frac{\pi}{2p_e} \end{cases} \quad p > 0. \quad (31)$$

The control output u_2 is calculated via the following formula:

$$u_2 = \frac{I_e}{c_2} \left[k_e \cdot s_e + d_e \cdot g(s_e) + e_{2e} \left(c_{1e} - c_{2e} \frac{b_e}{I_e} \right) + c_{2e} f_{2e} \right]. \quad (32)$$

3.4. Switching Control of Engine Demand Torque in the Engaging Process after Synchronizing. When engine speed and clutch driven plate speed approach to synchronizing and

reach set threshold values according to switching conditions, DCT launch models switch over; namely, the two-DOF sliding friction model transforms into the single-DOF 1st speed gear stable operated model. At the moment, the controller of sliding friction process does not work any longer. And switching controller of demand torque begins to work, which is in charge of converting engine torque into driver demand torque. It satisfies

$$T_e^d = T_e^L + K_e t, \quad (33)$$

$$K_e = \left(\frac{T_e^d - T_e^L}{\Delta t} \right), \quad (34)$$

wherein T_e^L is real engine torque at the switching moment of DCT launch models, T_e^d is driver demand torque, K_e is changing slope of engine torque, and Δt is switching time elapsed of demand torque.

In order to meet the requirement of vehicle shock intensity in the switching process, Δt has a minimum value. According to the 1st speed gear stably operated model (formula (8)), shock intensity is proportional to the changing rate of engine torque regardless of driving resistance and friction damping. That is

$$j = \frac{i_e R_W}{I_d} \dot{T}_e. \quad (35)$$

According to the requirement of shock intensity in the launching process, namely, $j \leq 10 \text{ m/s}^3$, the upper limited value of changing rate of engine torque can be calculated. The minimum time elapsed in the switching process of torque also can be obtained on the basis of formula (33).

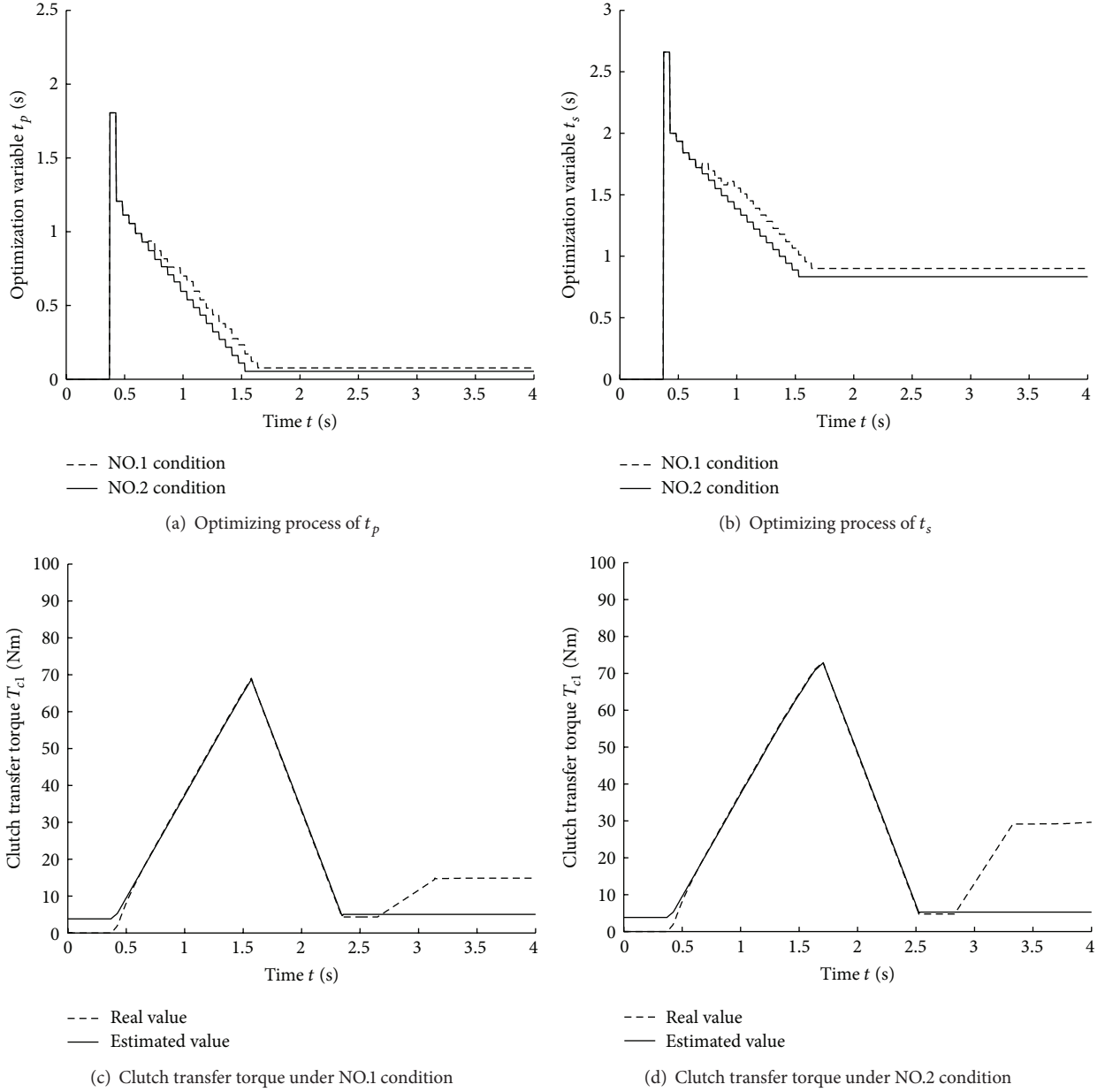


FIGURE 10: Comparisons of results of rolling optimization under NO.1 and NO.2 condition.

Similarly, according to the two-DOF launch model (Formula (5)) in the launch sliding friction process, we know that vehicle shock intensity in the sliding friction process is proportional to the changing rate of clutch transfer torque regardless of driving resistance and friction damping. So there is

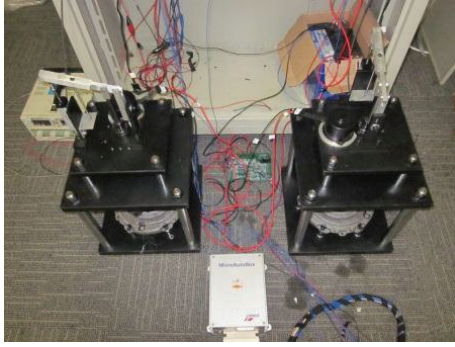
$$j = \frac{i_e R_W}{I_0} \dot{T}_{c1}. \quad (36)$$

4. Simulation Results and Analysis

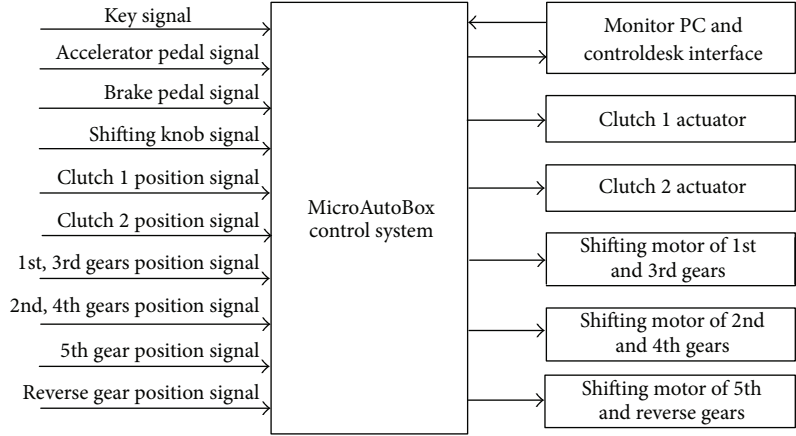
Based on the previously established dynamic model of dry DCT and its launch controller, the launch simulation model

of vehicle equipped with dry DCT is built on the Matlab/simulink software platform. Immediately, the performance of vehicle is simulated under typical launch condition. The detailed parameters of adopted DCT can be seen in the appendix.

Figure 9 and Table 3 demonstrate simulation results of launch condition, which are defined as that the changing rate of accelerator pedal angle is constant and that the final values are different. It means that changing rate of accelerator is 0.4 s^{-1} and that the final values are 20% and 40% respectively. Relatively, they are called NO.1 and NO.2 conditions respectively, which are shown in Figure 9(a). Compared with NO.4 condition (it reaches the final value at 1 s), NO.3 condition requires a slower launch process.



(a) Photo of dry DCT test bench



(b) Interfaces of DCT prototyping controller

FIGURE 11: DCT test bench and prototyping controller.

TABLE 3: Comparisons of simulated results of NO.1 and NO.2 conditions.

Working condition	NO.1	NO.2
Time elapsed when clutch driving and driven plates are synchronized t_s/s	2.355	2.535
Vehicle velocity when clutch driving and driven plates are synchronized $v/(km/h)$	8.1052	9.6367
Time elapsed when the demand torque switch over $(t_s + \Delta t)/s$	3.14	3.33
Vehicle velocity when the demand torque switch over $v/(km/h)$	8.3558	10.371
Total slipping friction work W/J	3739.9	4767.3
Time elapsed for launch t/s	3.14	3.33

In Figures 9(b), 9(c), and 9(g) and Table 3, both the synchronizing moment of clutch driving and driven plates and the switching finishing moment under NO.1 condition are earlier than that of NO.2 working condition. At any moment, vehicle velocity is quite little under NO.1 condition. So it can be concluded that the designed launch controller can reflect the driving intention. In Figures 9(d) and 9(e), launch impact strengths are less than 10 m/s^3 , which meet the demands. In Figures 9(f) and 9(g), engine output and clutch transfer torque can also be divided into five parts.

Figures 10(a) and 10(b) demonstrate optimal time variables t_p and t_s calculated at every rolling optimization. The total optimizing frequency is 22 under NO.1 condition, while the time elapsed is 1.53 s at the last optimization. Relatively, the total optimizing frequency is 24 times under NO.2 condition, while the time elapsed is 1.64 s at the last optimization. Figures 10(c) and 10(d) show that estimated value of T_{c1} is quite approaching to its real value in the launch sliding friction process. It ensures that sliding friction is least in the launching process to some degree.

5. Rapid Prototyping Experiments for Dry DCT in the Launching Process

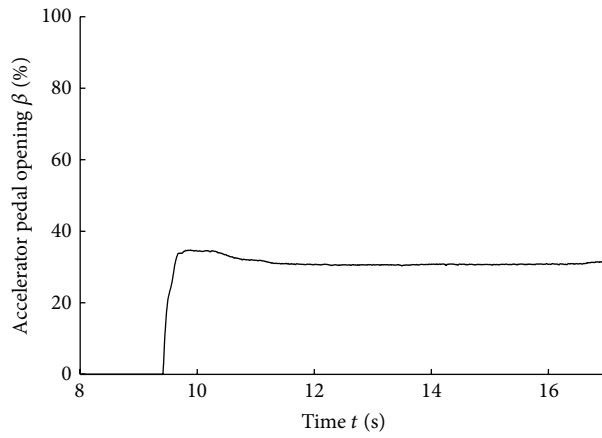
5.1. Five-Speed Dry DCT Transmission Actuator. In order to shorten the development cycle of dry DCT control system and test the real-time property and effectiveness of sliding mode variable structure control algorithm as well, the research group has established a dry DCT test bench (shown in Figure 11(a)) and used MicroAutoBox1401 of dSPACE Corporation as prototype controller. Some models are set up, such as five-speed dry DCT vehicle models (including engine mean value model, DCT model, and vehicle longitudinal dynamics model) and DCT control strategy model. The rapid prototyping experiments are conducted at the same time.

The interfaces of dry DCT prototype controller are shown in Figure 11(b). Before testing, calibrate the signals of sensors firstly and test the working performance of actuator motor driving units and actuator mechanisms in an open loop in order to ensure the reliability of hardware system. Secondly, test and verify the coordinating control strategy of clutch torque in a closed-loop. Thirdly, conduct the rapid prototyping experiments of sliding mode variable structure upper coordinating control strategy after proving its effectiveness and calibrating relative control parameters.

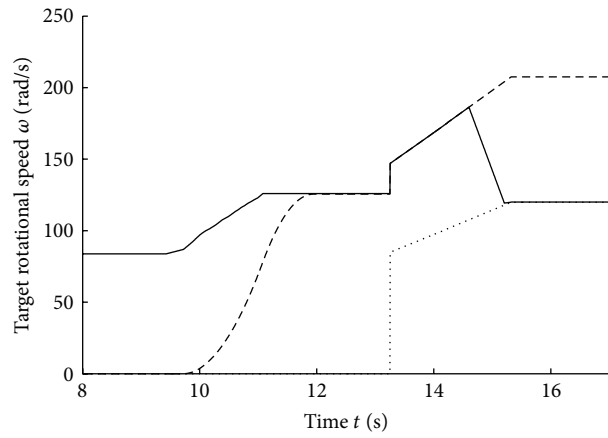
5.2. Results and Analysis of Rapid Prototyping Tests. By means of making use of RTI1401 toolbox offered by dSPACE Corporation, defining input signal pins such as accelerator pedal signal, brake pedal signal, and contacting with the previously designed DCT launch upper control module, the upper controller can be established.

The launch trigger signal is defined as follows: when the current speed gear is 1st speed gear, the brake pedal signal is zero (in loose state). The accelerator pedal opening is more than or equal to 3%. A trigger signal for preselecting 2nd speed gear is delayed 0.5 s after the launch is finished.

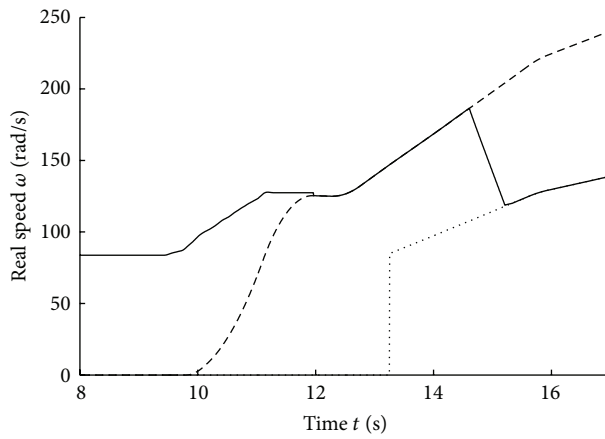
The trigger signal of shifting 1st speed gear to the 2nd one can be defined as follows: when the vehicle velocity is bigger



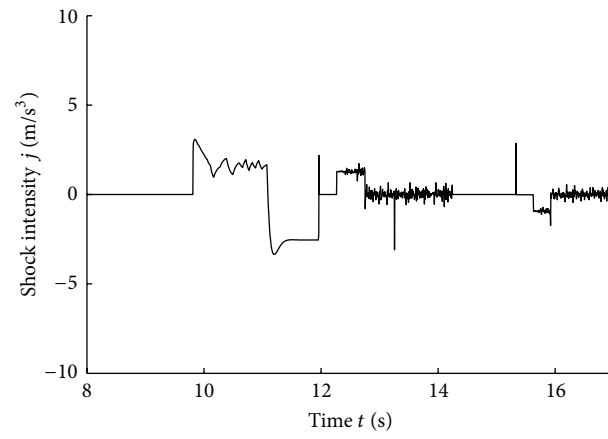
(a) Acceleration pedal opening



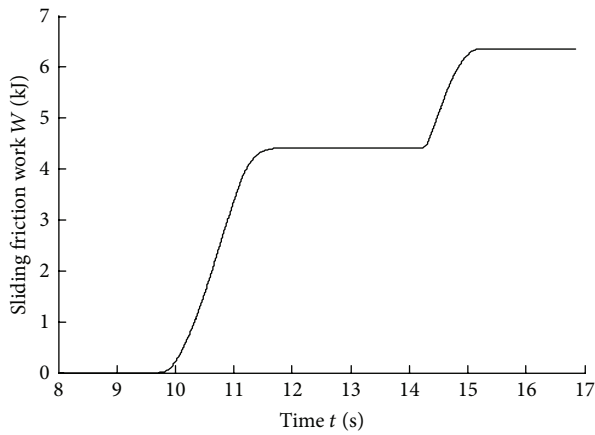
(b) Target rotational speed



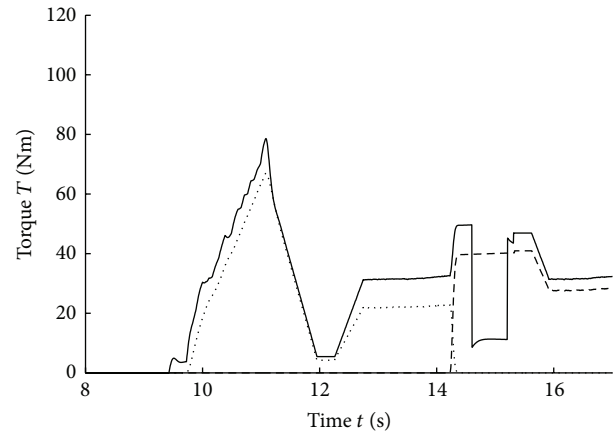
(c) Real rotational speed



(d) Shock intensity



(e) Sliding friction work



(f) Torque

FIGURE 12: Continued.

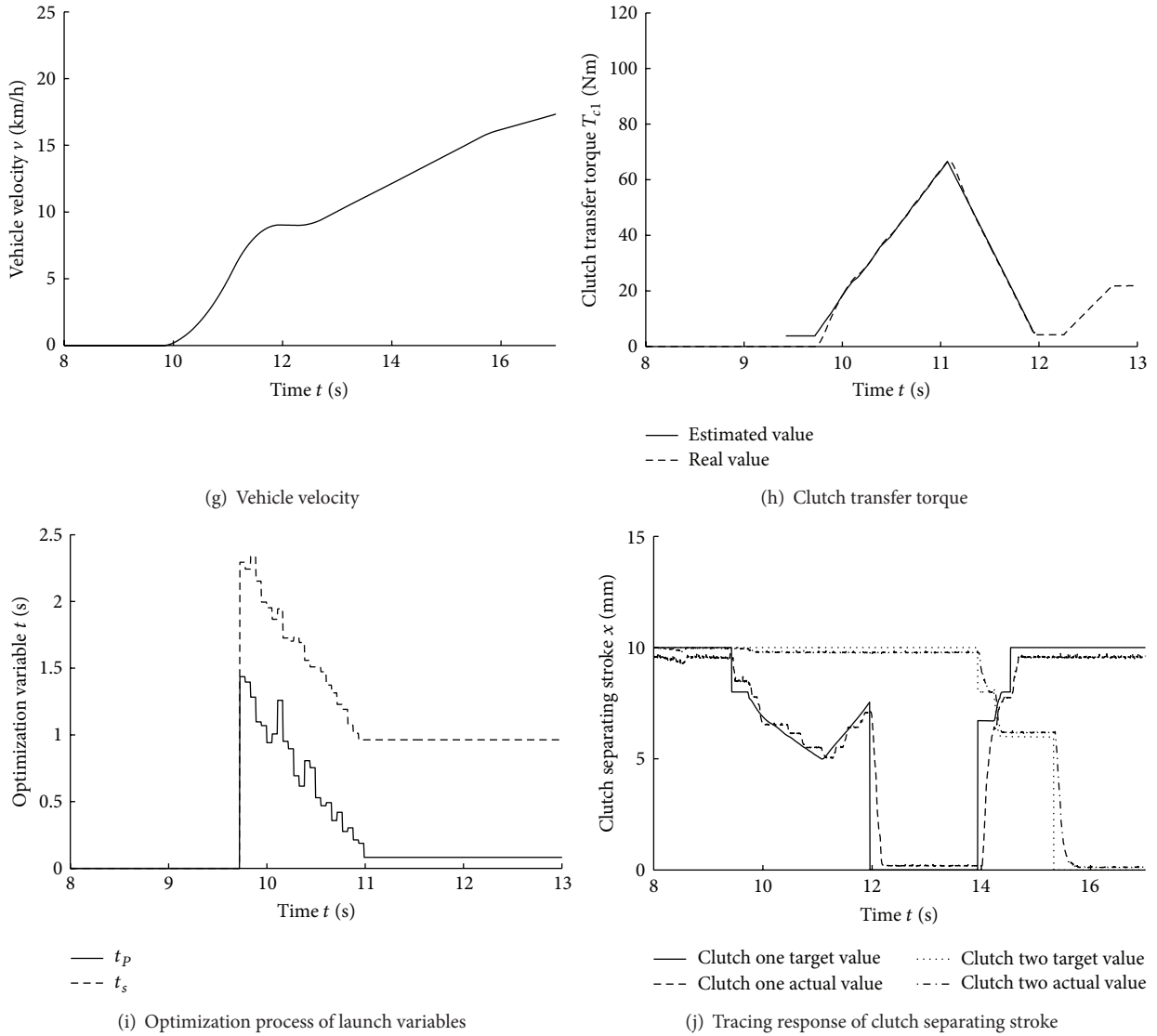


FIGURE 12: Rapid prototyping experiment results of launch and shifting from the 1st gear to the 2nd one.



FIGURE 13: Photo of real car chassis dynamometer test.

TABLE 4: Rapid prototyping experiment results of dry DCT in the launching process.

Launch moment t_0/s	9.425
Synchronizing moment of launch clutch 1 driving and driven plates $(t_0 + t_s)/s$	11.96
Vehicle velocity at the synchronizing moment of clutch 1 $v/(km/h)$	9.029
Switching finishing moment of launch demand torque $(t_0 + t_s + \Delta t)/s$	12.74
Vehicle velocity at the switching finishing moment of demand torque $v/(km/h)$	9.498
Total sliding friction work W/J	4416
Rolling optimization frequency of time variable	24
Time elapsed for launch t/s	3.315

than the 1st to 2nd gear shifting speed 12 km/h and the target gear is 2nd gear.

The rapid prototyping experiment results of upper controller are demonstrated in Figure 12 and Table 4. It can

be seen that the performance indexes of shock intensity and sliding friction work meet the standard demands in

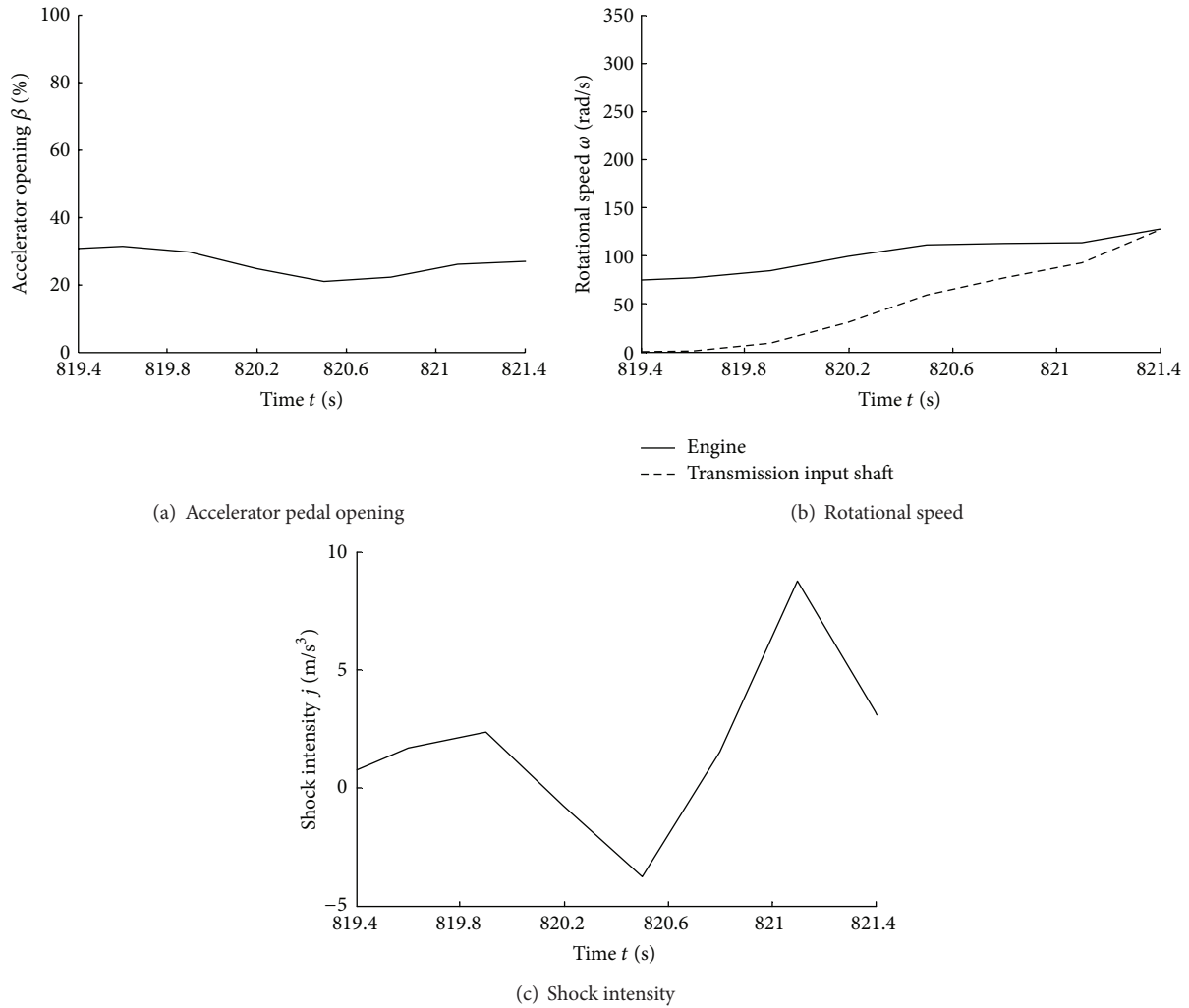


FIGURE 14: Results of dry DCT prototype car chassis dynamometer test.

the launching process and that results of rapid prototyping experiments coincide with simulated results. It is also proved that the stated sliding mode variable structure dry DCT upper controller can meet the requirement of real-time control based on real-time optimization.

6. Chassis Dynamometer Test of Real Car Equipped with Dry DCT

After rapid prototyping experiments, the independently developmental five-speed dry DCT control unit is used to replace the MicroAutoBox1401 rapid prototype controller. On the basis of simulation and bench test results, the corresponding MAP of prototype car equipped with dry DCT is recalibrated. After DCT software is developed, the real car chassis dynamometer test is conducted. The test photo is shown in Figure 13.

The results of launch test can be seen in Figure 14. The experiment results demonstrate that on the basis of sliding

mode variable structure upper coordinating control strategy, the developed dry DCT control software not only reflects the launch riding comfort of vehicle, but also reflects the variation of driver's intention.

As can be seen from Figure 14, under the proposed launching strategies, the vehicle is launched within 2 s and the shock intensity is below $10 m/s^3$. Besides, when the accelerator pedal opening is increasing, the corresponding shock intensity is relatively larger, which is consistent with the control strategies. Compared with the rapid prototyping tests, the results obtained in the chassis dynamometer test are also consistent, thus validating the effectiveness of the proposed control strategies.

7. Conclusion

The four-DOF launch dynamics model of five-speed dry DCT is established. After simplifying the model, two-DOF sliding friction model and single-DOF in-gear operation model are obtained, which provide a basis for the design and control

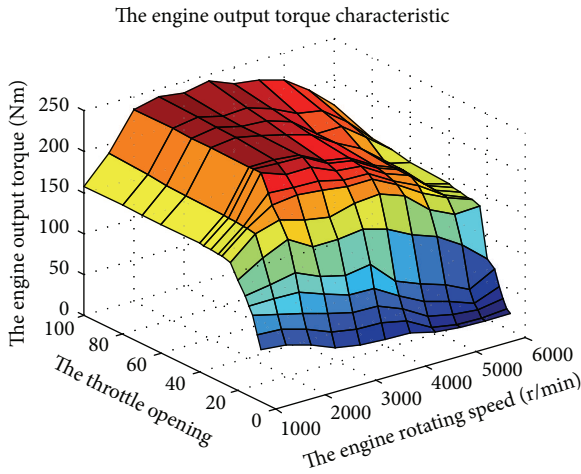


FIGURE 15

TABLE 5: The parameters of adopted DCT.

Parameters	Value
I_e	0.273 kg·m ²
I_{c1}	0.014 kg·m ²
I_{c2}	0.014 kg·m ²
I_m	0.01 kg·m ²
I_s	147.0392 kg·m ²
$I_{g1} \sim I_{g5}$	0.005 kg·m ²
I_{gr}	0.005 kg·m ²
$i_1 \sim i_5$	3.615, 2.042, 1.257 0.909, 0.714
i_a	3.895
b_e	0.01
b_{c1}	0.01
b_{c2}	0.01
b_m	0.01
b_s	0.01
m	1550 kg
f	0.0137
g	9.8 m/s ²
A	2.095 m
C_d	0.293
R_w	0.308 m
η	0.92
R_0	0.228 m
R_1	0.15 m

of launch controller. Driver's intention is reflected by using engine speed and vehicle shock intensity. Taking advantage of the idea of predictive control and genetic algorithm, the tracing curves of engine speed and vehicle target velocity are determined by rolling optimization online. The sliding mode variable structure controller (SMVS) is designed. Launch simulating model is built on the MATLAB/Simulink software platform for the dry DCT. the launch rapid prototyping

experiment is conducted. Simulation and experiment results show that the designed SMVS coordinating controller can effectively reflect the driver's intention and improve the vehicle's launch performance. Furthermore, chassis dynamometer test result of DCT prototype car also shows that the proposed SMVS launch coordinating control strategy is effective and feasible.

Appendices

A. The Engine Output Characteristics (Map)

See Figure 15.

B. The Parameters of Adopted DCT in This Paper

See Table 5.

Conflict of Interests

The authors declare that there is no conflict of interests regarding the publication of this paper.

References

- [1] D. Qin, Y. Liu, J. Hu, and R. Chen, "Control and simulation of launch with two clutches for dual clutch transmissions," *Chinese Journal of Mechanical Engineering*, vol. 46, no. 18, pp. 121–127, 2010.
- [2] D. Qin and Q. Chen, "Universal clutch starting control of AMT/DCT automatic transmission based on optimal control," *Chinese Journal of Mechanical Engineering*, vol. 47, no. 12, pp. 85–91, 2011.
- [3] C. Sun and J. Zhang, "Optimal control applied in automatic clutch engagements of vehicles," *Chinese Journal of Mechanical Engineering*, vol. 17, no. 2, pp. 280–283, 2004.
- [4] Q.-H. Chen, D.-T. Qin, and X. Ye, "Optimal control about AMT heavy-duty truck starting clutch," *China Journal of Highway and Transport*, vol. 23, no. 1, pp. 116–121, 2010.
- [5] F. Garofalo, L. Glielmo, L. Iannelli et al., "Optimal tracking for automotive dry clutch engagement," in *Proceedings of the International Federation of Automatic Control (IFAC '02)*, pp. 367–372, 2002.
- [6] I. A. Amir, D. T. Qin, and J. J. Liu, "A control strategy on launch up a vehicle with AMT," *Information Technology Journal*, vol. 4, no. 2, pp. 140–145, 2005.
- [7] G. Lucente, M. Montanari, and C. Rossi, "Modelling of an automated manual transmission system," *Mechatronics*, vol. 17, no. 2-3, pp. 73–91, 2007.
- [8] A. Serrarens, M. Dassen, and M. Steinbuch, "Simulation and control of an automotive dry clutch," in *Proceedings of the 2004 American Control Conference (AAC '04)*, pp. 4078–4083, July 2004.
- [9] C. H. Yu, H. Y. Chen, and H. R. Ding, "A study on fuzzy control of AMT clutch in launch phase," *Automotive Engineering*, vol. 27, no. 4, pp. 423–426, 2004.
- [10] Z. Qi, Q. Chen, and A. Ge, "Fuzzy control of the AMT vehicle's starting process based on genetic algorithm," *Chinese Journal of Mechanical Engineering*, vol. 37, no. 4, pp. 8–24, 2001.

- [11] M. Yong, D. Y. Sun, D. T. Qin et al., "Research on partial fuzzy control of car clutch in launch phase," *Automotive Technology*, vol. 12, pp. 12–15, 2008.
- [12] H. Kong, F. Ren, and Y. M. Ren, "Application of the genetic algorithm to optimizing fuzzy control strategy in the vehicle's launch process," *Journal of Hefei University of Technology*, vol. 32, no. 1, pp. 21–23, 2009.
- [13] M. X. Wu, J. W. Zhang, T. L. Lu et al., "Research on optimal control for dry dual-clutch engagement during launch," *Journal of Automobile Engineering*, vol. 224, no. 6, pp. 749–763, 2010.
- [14] G. Q. Wu and D. M. Zhan, "A research on the way of clutch actuation during DCT upshift based on optimality theory," *Automotive Engineering*, vol. 31, no. 3, 2009.
- [15] Y. Li, Z. Zhao, and T. Zhang, "Research on optimal control of twin clutch engagement pressure for dual clutch transmission," *China Mechanical Engineering*, vol. 21, no. 12, pp. 1496–1501, 2010.
- [16] W. Yang, Q. Chen, G. Wu, and D. Qin, "Starting control strategy for dual clutch transmission based on intelligent control and the performance simulation," *Chinese Journal of Mechanical Engineering*, vol. 44, no. 11, pp. 178–185, 2008.
- [17] Y. Liu, D. Qin, H. Jiang, and Y. Zhang, "A systematic model for dynamics and control of dual clutch transmissions," *Journal of Mechanical Design, Transactions of the ASME*, vol. 131, no. 6, pp. 0610121–0610127, 2009.
- [18] Y. S. Zhao, *Integrated control of dual clutch transmission system [M.S. thesis]*, Chongqing University.
- [19] H.-O. Liu, H.-Y. Chen, H.-R. Ding, and Z.-B. He, "Adaptive clutch engaging process control for automatic mechanical transmission," *Journal of Beijing Institute of Technology*, vol. 14, no. 2, pp. 170–174, 2005.
- [20] F. Garofalo, L. Glielmo, L. Iannelli et al., "Smooth engagement for automotive dry clutch," in *Proceedings of the IEEE Control Systems Society Conference*, vol. 1, pp. 529–534, 2001.



Hindawi

Submit your manuscripts at
<http://www.hindawi.com>

